Original Article

Value of ^{18}F-FDG PET/CT for differentiating diagnosis between malignant and benign primary gastric gastrointestinal mesenchymal tumors: a single-center retrospective study

Shengxu Li, Duanyu Lin, Mingdeng Tang, Daojia Liu, Qinghu Lyu, Jieping Zhang

Department of Nuclear Medicine, Fujian Medical University Cancer Hospital & Fujian Cancer Hospital, Fuzhou, China

Contributions: (I) Conception and design: S Li, D Lin; (II) Administrative support: M Tang; (III) Provision of study materials or patients: S Li, Q Lyu; (IV) Collection and assembly of data: S Li, J Zhang; (V) Data analysis and interpretation: S Li, D Liu; (VI) Manuscript writing: All authors; (VII) Final approval of manuscript: All authors.

Correspondence to: Duanyu Lin. Department of Nuclear Medicine, Fujian Medical University Cancer Hospital & Fujian Cancer Hospital, No. 420 Fuma Road, Jinan District, Fuzhou 350014, China. Email: lindy120@163.com.

Background: Malignant primary gastric gastrointestinal stromal tumors (gGISTs) without treatment with imatinib are prone to bleeding and peritoneum implantation during operation. Therefore, preoperative assessment of the malignant potential of gGIST is essential. The use of ^{18}F-fluorodeoxyglucose (^{18}F-FDG) positron emission tomography (PET) combined with computed tomography (PET/CT) as a non-invasive tool for diagnosis, staging and prognosis evaluation in oncology, may also be useful for gGISTs. In the present study, we analyzed the value of ^{18}F-FDG PET-CT in assessing the malignant potential of gGISTs before treatment.

Methods: Patients who were diagnosed with gGIST by pathology and underwent ^{18}F-FDG PET/CT at the same time were collected. The clinicopathological features of 26 patients with gGISTs were retrospectively analyzed at last. The gGIST risk classification was graded according to the US National Institutes of Health (NIH) GIST risk classification criteria [2008]. Lesions were classified as malignant group (moderate- or high-risk category) and benign group (low- or very low-risk category) according to pathology. The relationship between the maximal standard uptake value (SUVmax) and GIST risk category, tumor diameter, Ki-67 index, and mitotic count was analyzed. The cut-off level of SUVmax for the diagnosis of malignant gGIST with the highest sensitivity was calculated based on the receiver-operating characteristic (ROC) curve.

Results: The SUVmax, tumor diameter, Ki-67 index, and mitotic count of the 26 gGIST patients were 5.90±4.49, 7.40±4.92 cm, 7.62%±11.76%, (5.96±3.19)/50 high-power field (HPF), respectively. SUVmax was significantly correlated with GIST risk category, Ki-67 index, and mitotic count (r=0.855, 0.860, and 0.690, all P<0.01) but not with tumor diameter (r=0.383, P=0.054). The SUVmax of gGIST was 7.00±4.57 in the malignant group (moderate or high NIH risk category in 20 patients), which was significantly different from that (2.25±0.77) in the benign group (low or extremely low NIH risk category in 6 patients) (t=4.566, P<0.01). ROC curve analysis showed that a SUVmax cut-off of 2.60 was most sensitive for predicting malignant gGIST. When the area under the curve was 0.967, the sensitivity was 100% and the specificity was 83.3%.

Conclusions: SUVmax may be used as a complementary indicator for predicting the malignant potential of gGISTs before treatment.

Keywords: Gastric gastrointestinal stromal tumors (gGISTs); ^{18}F-fluorodeoxyglucose (^{18}F-FDG); positron emission tomography (PET); risk classification; maximum standardized uptake value (SUVmax)

Submitted Jan 27, 2022. Accepted for publication Apr 13, 2022.

doi: 10.21037/jgo-22-287

View this article at: https://dx.doi.org/10.21037/jgo-22-287

Introduction

Gastrointestinal stromal tumors (GISTs) are the most common mesenchymal tumor of the gastrointestinal tract, accounting for 3% of all gastrointestinal tract tumors. Approximately 60% of GISTs originate in the stomach (1,2). Surgery remains the preferred treatment for gastric GISTs (gGISTs) (3-5). According to National Comprehensive Cancer Network (NCCN) guidelines, close follow up is sufficient for gGISTs that <2 cm and have no risk factors (6). However, intermediate-/high-risk disease is still found in patients with gGISTs ≤2 cm, indicating the diversity and complexity of the biologic behavior of gGISTs (7). In 2008, the US National Institutes of Health (NIH) revised its risk classification criteria of GISTs (8). Risk category was determined by the tumor size, mitotic index, and primary site, and the mitotic count must be acquired by surgery or biopsy. In some patients, however, tumors are difficult to biopsy or the amount of biopsied tissue is too small for mitotic counting, and tumor dissemination can occur due to bleeding during biopsy. Therefore, pretreatment assessment of the biologic behavior of gGISTs can be somehow difficult. Some anatomic imaging techniques can be used to predict the preoperative malignant potential of gGISTs, such as endoscopic ultrasonography (EUS), computed tomography (CT), magnetic resonance imaging (MRI) and ^{18}F-fluorodeoxyglucose (^{18}F-FDG) positron emission tomography (PET) combined with computed tomography (PET/CT). EUS can detect submucosal neoplastic lesions well, but it is hard to judge subserosa, deep abdominal lesions and their surrounding conditions. Preoperative contrast-enhanced CT may be helpful in predicting pathologic risk categories of GISTs and multi-parameter MR analysis provides a preoperative imaging standard for accurately distinguishing very low-to-low-risk GIST from intermediate-to-high-risk GIST, which was reported by Grazzini *et al.* (9) and Zheng *et al.* (10) respectively. However, they are relatively complex and do not form a universally applicable standard. ^{18}F-FDG PET/CT is a non-invasive and convenient imaging tool that integrates functional imaging and anatomical imaging. In the present study, we assessed the malignant potential of gGISTs by using ^{18}F-FDG PET/CT. We present the following article in accordance with the STARD reporting checklist (available at https://jgo.amegroups.com/article/view/10.21037/jgo-22-287/rc).

Methods

General clinical data

The present study was approved by the Medical Ethics Commission of Fujian Medical University Cancer Hospital (No. K2022-021-01). The clinical and imaging data of 34 gGIST patients who visited our hospital for the first time between January 2011 and December 2018 and underwent ^{18}F-FDG PET/CT were collected. Four patients had received treatment before the examination and the other four did not undergo surgical resection and were therefore excluded. A total of 26 patients were used in the final analysis. Of these patients, 13 were males and 13 were females and aged 60.85±9.37 years. ^{18}F-FDG PET/CT was completed within 1 week before surgery. Tumors in these 26 patients were completely resected. Clinical manifestations included abdominal pain and discomfort, abdominal mass, dysphagia, and hematemesis/black stool. The study was conducted in accordance with the Declaration of Helsinki (as revised in 2013). Individual consent for this retrospective analysis was waived.

Clinical research design

We analyzed the relationship between the maximal standard uptake value (SUVmax) and GIST risk category, tumor diameter, Ki-67 index, and mitotic count. Due to the small sample size, the deviation of the results may occur. The area under the receiver operating characteristic (ROC) curve was used to determine the SUVmax cut-off level able to predict tumor malignant potential with the highest sensitivity.

Imaging

The Gemini TF 64 PET/CT instrument (Philips Healthcare, Cleveland, Ohio, USA) was used. ^{18}F-FDG was generated from HM-10 cyclotron (Sumitomo, Japan), with a radiochemical purity of >95%. Before the examination, patients fasted for >6 h, and blood glucose levels were controlled in the range of 3.9–7.5 mmol/L. After intravenous injection of 185–370 MBq of ^{18}F-FDG, patients were asked to rest for 60 min. After urination, the patients were scanned in the supine position. The CT acquisition parameters were 120 kV, 200 mA, matrix 512×512, and layer thickness 5 mm. Patients were scanned from the base of the

skull to the upper thigh, and the PET images were acquired in 3D mode with 1 min/bed position. CT data were used for attenuation correction. The PET and CT images were fused on a Philips EBW workstation to obtain the PET, CT, and fused PET/CT images on the transverse, sagittal, and coronal planes.

Image analysis

PET, CT, and fused PET/CT images were evaluated by 2 senior nuclear medicine doctors who have more than 10 years diagnostic experience using the double-blind method. The level with the highest radioactivity uptake was selected on the cross-sectional image. With 90% of the lesion as the region of interest (ROI), the maximum standard uptake value (SUVmax) was automatically calculated using a computer, and the results were judged by the boundary, morphology, and density of the lesions.

Pathological of gGISTs

Tumor specimens obtained by surgical resection were fixed in 10% formaldehyde, embedded in paraffin and stained with hematoxylin and eosin for pathological evaluation of the mitotic index, which indicates the number of mitotic cells per 50 high-power fields (HPFs) or per 5 mm^2 fields. Immunohistochemical staining for CD117, DOG1, CD34, SDHB, smooth muscle actin and S-100 was performed by the standard avidin-biotin peroxidase complex method. The Ki-67 index was defined as the percentage of nuclear stained tumor cells per 1,000 tumor cells. Molecular detection includes c-KIT or PDGFRA mutation analysis.

GIST risk classification criteria

The risk category of gGIST was determined pathologically based on the tumor size and the number of mitotic cells in accordance with the US NIH GIST risk classification criteria [2008]. The details of the risk category have been described in a previous report (8). Lesions were classified as malignant group (moderate- or high-risk category) and benign group (low- or very low-risk category) according to pathology.

Statistical analysis

Statistical analysis was performed using SPSS 22.0 (IBM, Armonk, NY, USA). Measurement data were compared using *t*-test, and correlation between the SUVmax and GIST risk category, tumor diameter, Ki-67 index, and mitotic count were performed using Pearson or Spearman methods. The cut-off value of SUVmax for the diagnosis of malignant gGIST with the highest sensitivity was calculated from the receiver-operating characteristic (ROC) curve. The optimal cutoff value was defined as the value of a parameter when the sum of sensitivity and specificity was maximized. Sensitivity = true positive/(true positive + false negative). Specificity = true negative/(false positive + true negative). $P<0.05$ was considered statistically significant.

Results

^{18}F-FDG PET/CT images and clinicopathological characteristics

^{18}F-FDG PET/CT images and clinicopathological characteristics of 26 gGIST patients are shown in *Tables 1*,*2*, respectively. Imaging features of a typical patient are shown in *Figure 1*.

Relationship between SUVmax and clinicopathological features

SUVmax, tumor diameter, Ki-67 index, and mitotic count of the 26 patients were 5.90±4.49, 7.40±4.92 cm, 7.62%±11.76%, and (5.96±3.19)/50 HPF. SUVmax was significantly correlated with GIST risk category, Ki-67 index, and mitotic count (r=0.855, 0.860, and 0.690, respectively; all $P<0.01$) but not with tumor diameter (r=0.383, P=0.054) (*Table 3*). The SUVmax of gGIST was 7.00±4.57 and 2.25±0.77 in the malignant group (20 patients who were moderate- or high-risk category) and benign group (6 patients who were low- or very low-risk category), respectively, showing statistically significant difference (t=4.566, $P<0.01$).

Value of SUVmax for diagnosing malignant gGIST

ROC curve analysis showed that, when the SUVmax threshold for diagnosing malignant gGIST was set at 2.60, the area under the curve was 0.967, with a sensitivity of 100% and a specificity of 83.3% (*Figure 2*).

Discussion

GISTs are tumors that occur mostly in the stomach,

Table 1 ^{18}F-fluorodeoxyglucose positron emission tomography/computed tomography findings of 26 patients with primary gastric gastrointestinal mesenchymal tumors

n	Sex	Age (years)	Site	Tumor diameter (cm)	SUVmax	Ki-67 (%)	Mitotic count (/50 HPF)	Necrosis	Bleeding	Cystic change	Risk category
1	Female	55	Gastric body	8.3	8.8	5	8	No	No	Yes	High
2	Female	70	Gastric body	15.0	5.9	8	11	Yes	Yes	No	High†
3	Female	60	Gastric body	15.0	5.8	2	11	Yes	Yes	No	High
4	Male	68	Gastric body	5.3	22.4	50	12	No	No	No	High
5	Female	67	Gastric body	8.8	4.2	8	5	No	Yes	No	High
6	Female	47	Fundus of stomach	15.0	8.3	10	6	No	No	No	High
7	Female	52	Fundus of stomach	13.8	10.4	40	10	Yes	No	No	High
8	Female	70	Fundus of stomach	9.0	10.8	15	11	No	Yes	No	High
9	Male	47	Gastric antrum	21.6	10.5	12	8	Yes	Yes	No	High
10	Male	52	Cardia	7.6	10.8	10	7	No	Yes	No	High
11	Female	64	Gastric body	6.0	2.9	2	5	Yes	No	No	Intermediate
12	Male	67	Gastric body	5.1	5.9	1	5	No	No	No	Intermediate
13	Male	66	Gastric body	8.5	4.9	2	5	No	Yes	No	Intermediate†
14	Female	77	Gastric body	5.9	2.8	1	2	No	No	No	Intermediate
15	Male	65	Gastric body	6.7	3.2	5	2	No	Yes	No	Intermediate
16	Female	51	Fundus of stomach	3.5	6.0	7	5	Yes	No	No	Intermediate
17	Male	54	Fundus of stomach	3.8	3.8	2	7	Yes	No	No	Intermediate
18	Female	40	Fundus of stomach	5.3	3.4	5	5	No	Yes	No	Intermediate
19	Female	75	Fundus of stomach	5.2	4.8	3	5	No	Yes	No	Intermediate
20	Male	59	Fundus of stomach	5.5	4.3	3	1	No	No	No	Intermediate
21	Male	51	Gastric body	3.0	2.4	1	1	No	No	No	Low
22	Male	66	Fundus of stomach	3.5	2.1	1	5	No	No	No	Low†
23	Female	61	Cardia	2.5	3.7	2	7	No	No	No	Low
24	Male	67	Cardia	2.5	2.0	1	5	No	No	No	Low
25	Male	69	Gastric antrum	5.0	1.8	1	1	No	No	No	Low
26	Male	62	Gastric body	1.1	1.5	1	5	No	No	No	Extremely low†

†, typical gastric gastrointestinal mesenchymal tumor. HPF, high-power field; SUVmax, maximal standard uptake.

Table 2 Clinical and pathological features of 26 patients with primary gastric gastrointestinal mesenchymal tumors

Clinicopathological features	n (%)
Sex	
Male	13 (50.0)
Female	13 (50.0)
Clinical manifestations	
Pain/discomfort	12 (46.2)
Physical examination findings	4 (15.4)
Abdominal mass	4 (15.4)
Dysphagia	3 (11.5)
Hematemesis or black stools	3 (11.5)
Primary tumor site	
Gastric body	12 (46.2)
Fundus of stomach	9 (34.6)
Gastric antrum	2 (7.7)
Cardia	3 (11.5)
Tumor diameter (cm)	
<2	1 (3.9)
2–5	7 (26.9)
5–10	13 (50.0)
>10	5 (19.2)
Mitotic count (/50 HPF)	
<6	15 (57.7)
6–10	7 (26.9)
>10	4 (15.4)
Risk category	
High	10 (38.5)
Intermediate	10 (38.5)
Low	5 (19.2)
Extremely low	1 (3.8)
CT features	
With accompanying necrosis, hemorrhage, and cystic change	15 (57.7)
Without accompanying signs	11 (42.3)

HPF, high-power field; CT, computed tomography.

especially in the body and fundus of the stomach. They mainly manifest as abdominal pain and abdominal mass, which could be accompanied by nausea, vomiting, or gastrointestinal bleeding (11). According to NCCN guidelines, gGISTs ≤2 cm have less aggressive biologic behavior and are considered low risk, therefore close follow up is recommended (6). For patients with larger tumors (>10 cm) or multiple lesions, preoperative treatment with imatinib is recommended as the first option, and total gastrectomy or combined organ resection should be avoided (12). Some patients with small GISTs can rapidly develop liver metastases (13), whereas patients with large GISTs generally remain disease free for long durations, without the need for postoperative adjuvant therapy (14). All of these reflect the uncertainty of the biologic behaviors of GISTs. With advancements in precision medicine, there is an increasing need for methods to differentiate the malignant potential of GISTs. Many parameters, including original tumor site, tumor size, mitotic count, and Ki-67 proliferation index, have been proposed to assess the malignant potential of GISTs, among which tumor size and mitotic count are most often used. Based on tumor size, mitotic count, and original site, the US NIH classification divided the biologic behaviors of GISTs into the following 4 groups of progression: high, intermediate, low, and very low risk. Tumor size and location can be obtained by conventional imaging, such as endoscopic ultrasound, enhanced CT, and magnetic resonance imaging. Mitotic count were assessed by invasive pathological examination. For GIST patients for whom biopsy tissues could not be easily obtained or only a very small amount of biopsy tissues could be harvested, mitotic count is difficult to determine in 50 consecutive HPFs, which increases the difficulty of GIST risk classification before treatment.

^{18}F-FDG PET/CT as a non-invasive imaging modality that integrates functional imaging and anatomical imaging is widely used in tumor staging, response evaluation, and prognostic prediction. In an era of molecular targeted therapy for tumors, ^{18}F-FDG PET/CT is particularly valuable in assessing the efficacy of targeted drugs (e.g., imatinib) in the treatment of GISTs (15,16).

SUVmax is a semiquantitative marker of tumor glucose metabolism detected by PET/CT and is based on the level of ^{18}F-FDG uptake. A higher SUVmax value indicates higher expression of glucose transporter protein and more active glycolysis in tumor cells, along with the more malignant nature of the tumor (17). In the current study, SUVmax was strongly correlated with gGIST risk category of ($r=0.855$, $P<0.01$), that is, a higher SUVmax was associated with more malignant potential of gGISTs, which was consistent with the published literature (18-22).

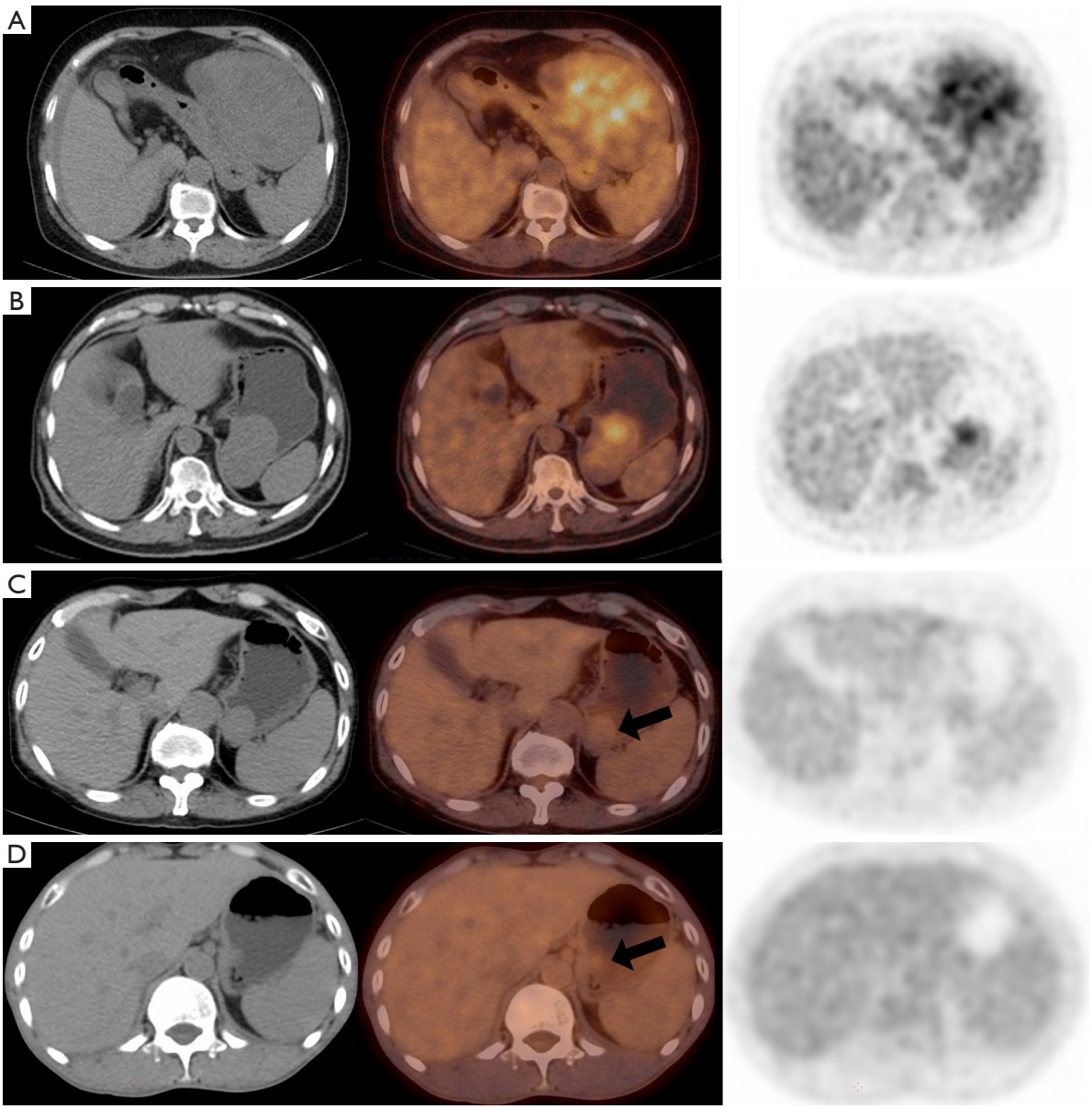

Figure 1 Typical gGIST. From left to right: CT imaging, fused PET/CT imaging, and PET imaging at the same cross-sectional level. (A) A 70-year-old female presented with recurrent epigastric pain and discomfort, and the lesion was pathologically confirmed as a mesenchymal tumor of the greater curvature of the gastric body (high-risk category). CT imaging showed exophytic growth pattern and uneven soft tissue density. PET/CT imaging showed high FDG uptake with SUV of 5.9. (B) A 66-year-old male presented with dysphagia, and the lesion was pathologically confirmed as a mesenchymal tumor of the gastric body (intermediate-risk category). CT imaging showed intracavity growth pattern and even soft tissue density. PET/CT imaging showed medium FDG uptake with SUV of 4.9. (C) A 66-year-old male presented with abdominal pain and discomfort, and the lesion was pathologically confirmed as a mesenchymal tumor of the gastric fundus (low-risk category). CT imaging showed intracavity growth pattern and even soft tissue density. PET/CT imaging showed low FDG uptake with SUV of 2.1. (D) A space-occupying mass was found during a health check-up of a 62-year-old male. It was pathologically confirmed as a mesenchymal tumor of the gastric body (extremely low-risk category). CT imaging showed intracavity growth pattern and even soft tissue density. PET/CT imaging showed very low FDG uptake with SUV of 1.5. The black arrow indicates the site of gGIST. gGIST, gastric gastrointestinal stromal tumor; CT, computed tomography; PET, positron emission tomography; FDG, fluorodeoxyglucose; SUV, standard uptake value.

Table 3 Relationships between SUVmax and clinicopathological features in 26 patients with primary gastric gastrointestinal mesenchymal tumors

Parameter	Correlation	SUVmax†	Tumor diameter†	Ki-67†	Mitotic count†	Risk category‡
SUVmax	Correlation	1	0.383	0.860	0.690	0.855
	P value		0.054	0.000	0.000	0.000
Maximum diameter	Correlation		1	0.288	0.498	0.871
	P value			0.153	0.010	0.000
Ki-67 index	Correlation			1	0.597	0.829
	P value				0.001	0.000
Mitotic count	Correlation				1	0.692
	P value					0.000
Risk category	Correlation					1
	P value					

†, Pearson correlation method; ‡, Spearman correlation method. SUVmax, maximal standard uptake value.

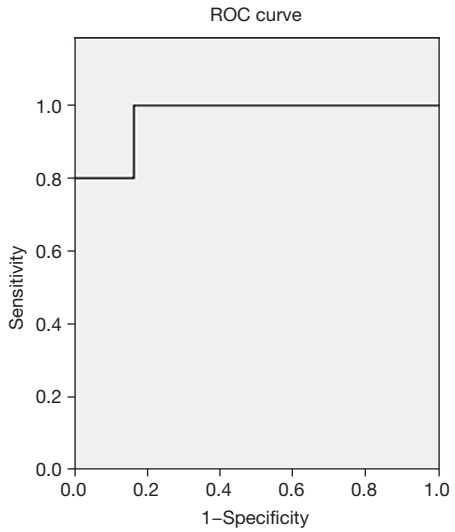

Figure 2 ROC curve of maximum standardized uptake value for the diagnosis of malignant gastric gastrointestinal mesenchymal tumors. ROC, receiver-operating characteristic.

Moreover, the SUVmax of GISTs in the malignant group was significantly higher than that in the benign group (7.00±4.57 *vs.* 2.25±0.77, t=4.566, P<0.01). In addition, ROC curve analysis showed that, when the SUVmax threshold for diagnosing malignant gGISTs was 2.60, it had a sensitivity of 100% and a specificity of 83.3% in the diagnosis of malignant potential. It was close to the SUVmax threshold (3.0) reported by Kamiyama *et al.* and Tokumoto *et al.* (18,22).

The proliferation-related nuclear antigen Ki-67 is a reliable indicator of cell proliferation. Research has shown that, using 6% as the threshold, Ki-67 >6% is associated with the high malignant potential of GIST, high risk of recurrence or metastasis, and poor prognosis (23). Zhao *et al.* showed that Ki-67 index >8% can be used to complement the modified NIH criteria in predicting the prognosis of GISTs, especially in identifying high-risk GIST patients with significantly poor prognosis (24). In our current series, there was a strong correlation between Ki-67 index and GIST risk category (r=0.829, P<0.01), indicating that the Ki-67 index can be used as an indicator to assess the malignant potential of gGISTs. In addition, SUVmax was strongly correlated with Ki-67 index (r=0.860, P<0.01), suggesting that SUVmax is also an effective predictor of the malignant potential of gGISTs, which is consistent with the literature (18-20).

Among the 3 traditional parameters (tumor diameter, mitotic count, and tumor site) used for GIST risk assessment, mitotic count was found to have the highest efficacy (25). In the current study, mitotic count was correlated with the GIST risk category (r=0.692, P<0.01), while SUVmax was correlated with mitotic count (r=0.690, P<0.01), indicating that SUVmax could predict the malignant potential of gGISTs, as demonstrated in Kamiyama *et al.*, Park *et al.*, and Yoshikawa *et al.*'s studies (18-20). While mitotic count is undoubtedly one of the most important parameters for GIST risk grading, the acquisition of mitotic count data in GIST patients before treatment requires a high-quality pathological

specimen. Furthermore, mitotic count measurement needs to be performed under 50 consecutive HPFs at the hotspots, which is associated with a high possibility of underestimation. Traditional counting techniques are limited by poor reproducibility; in addition, because of the heterogeneity of tumors, proliferative activity could differ significantly among different parts of the tumor, and the mitotic counts acquired can be highly diverse in the selected areas. Although Choi *et al.* found pathological uniformity between the periphery and center of GISTs (26), the tumors were small (3.56±2.10 cm) and had homogeneous growth, with few necrotic or cystic changes. In the clinical setting, the ^{18}F-FDG uptake often differs among different parts within the same GIST. Therefore, whether there are differences in the pathological features obtained at different sites of the same lesion also needs to be further validated in large-sample studies. All these factors can affect the results of GIST risk classification. SUVmax in our current study was positively correlated with mitotic count. Because SUVmax can be obtained by non-invasive ^{18}F-FDG PET-CT before treatment, it could be used as a complementary indicator for predicting the malignant potential of gGISTs.

Tumor diameter is another important parameter for GIST risk classification. In the current study, however, SUVmax was not correlated with tumor diameter (r=0.383, P=0.054), which was consistent with the findings of Kamiyama *et al.* and Yoshikawa *et al.* (18,20), but not with those of Cho *et al.* and Tokumoto *et al.* (21,22). Interestingly, Tokumoto *et al.* revealed only a weak correlation between SUVmax and tumor diameter (r=0.0441, P=0.021) (22). A possible explanation for this could be that some very small GISTs can progress rapidly and spread distantly (13). Lasota *et al.* demonstrated that GISTs with platelet-derived growth factor receptor alpha, (PDGFRA) gene mutation mostly occur in the stomach (27). Although these GISTs tend to develop into larger tumors, they have benign or less malignant biologic behaviors. Therefore, the biologic behaviors of GISTs are highly complex and unpredictable. It is also possible that cells in some parts of a GIST can grow rapidly to form a large tumor, whose nutritional needs are not be met by the limited blood supply, leading to the formation of cystic/necrotic changes. Due to insufficient blood supply, ^{18}F-FDG cannot efficiently reach tumor cells. The number of surviving tumor cells in necrotic tumor tissue is low, leading to the reduced uptake of ^{18}F-FDG. As a result, a large tumor could have a low SUVmax, which again reflects the complexity of the biologic behavior of GISTs. Furthermore, some GISTs do not grow uniformly, and measuring the malignant potential of tumors by diameter or maximum diameter alone is insufficient. Tumor metabolic volume could be considered as a good alternative indicator (28).

As the biologic behaviors of GISTs are diverse, GIST risk classification using only a few simple parameters is often inadequate in clinical practice. Individualized tumor treatment requires more diversified assessment of GIST malignant potential. The current study was limited by its small sample size (especially the small number of cases with low- or very low-risk categories) and the retrospective single-center design. Future multicenter studies with larger sample sizes are warranted.

In conclusion, ^{18}F-FDG PET/CT is a non-invasive and convenient imaging tool that integrates functional imaging and anatomical imaging. A single scan can obtain local tumor information, including tumor size and primary site, as well as the presence of distant metastases, if any. Its semiquantitative indicator, SUVmax, correlates with GIST risk category, Ki-67 index, and mitotic count, and may therefore be used as an effective complementary indicator for predicting the malignant potential of gGISTs before treatment.

Acknowledgments

Funding: None.

Footnote

Reporting Checklist: The authors have completed the STARD reporting checklist. Available at https://jgo.amegroups.com/article/view/10.21037/jgo-22-287/rc

Data Sharing Statement: Available at https://jgo.amegroups.com/article/view/10.21037/jgo-22-287/dss

Conflicts of Interest: All authors have completed the ICMJE uniform disclosure form (available at https://jgo.amegroups.com/article/view/10.21037/jgo-22-287/coif). The authors have no conflicts of interest to declare.

Ethical Statement: The authors are accountable for all aspects of the work in ensuring that questions related to the accuracy or integrity of any part of the work are appropriately investigated and resolved. The study was conducted in accordance with the Declaration of Helsinki (as revised in 2013). The study was approved by Medical

Ethics Commission of Fujian Medical University Cancer Hospital (No. K2022-021-01). Individual consent for this retrospective analysis was waived.

References

1. Gayed I, Vu T, Iyer R, et al. The role of 18F-FDG PET in staging and early prediction of response to therapy of recurrent gastrointestinal stromal tumors. J Nucl Med 2004;45:17-21.
2. DeMatteo RP, Lewis JJ, Leung D, et al. Two hundred gastrointestinal stromal tumors: recurrence patterns and prognostic factors for survival. Ann Surg 2000;231:51-8.
3. Blay JY, Bonvalot S, Casali P, et al. Consensus meeting for the management of gastrointestinal stromal tumors. Report of the GIST Consensus Conference of 20-21 March 2004, under the auspices of ESMO. Ann Oncol 2005;16:566-78.
4. Casali PG, Abecassis N, Aro HT, et al. Gastrointestinal stromal tumours: ESMO-EURACAN Clinical Practice Guidelines for diagnosis, treatment and follow-up. Ann Oncol 2018;29:iv68-78.
5. Poveda A, García Del Muro X, López-Guerrero JA, et al. GEIS guidelines for gastrointestinal sarcomas (GIST). Cancer Treat Rev 2017;55:107-19.
6. von Mehren M, Kane JM, Bui MM, et al. NCCN Guidelines Insights: Soft Tissue Sarcoma, Version 1.2021. J Natl Compr Canc Netw. 2020;18:1604-12.
7. Miettinen M, Sobin LH, Lasota J. Gastrointestinal stromal tumors of the stomach: a clinicopathologic, immunohistochemical, and molecular genetic study of 1765 cases with long-term follow-up. Am J Surg Pathol 2005;29:52-68.
8. Joensuu H. Risk stratification of patients diagnosed with gastrointestinal stromal tumor. Hum Pathol 2008;39:1411-9.
9. Grazzini G, Guerri S, Cozzi D, et al. Gastrointestinal stromal tumors: relationship between preoperative CT features and pathologic risk stratification. Tumori 2021;107:556-63.
10. Zheng T, Du J, Yang L, et al. Evaluation of risk classifications for gastrointestinal stromal tumor using multi-parameter Magnetic Resonance analysis. Abdom Radiol (NY) 2021;46:1506-18.
11. Bamboat ZM, Dematteo RP. Updates on the management of gastrointestinal stromal tumors. Surg Oncol Clin N Am 2012;21:301-16.
12. Al-Share B, Alloghbi A, Al Hallak MN, et al. Gastrointestinal stromal tumor: a review of current and emerging therapies. Cancer Metastasis Rev 2021;40:625-41.
13. Tanaka J, Oshima T, Hori K, et al. Small gastrointestinal stromal tumor of the stomach showing rapid growth and early metastasis to the liver. Dig Endosc 2010;22:354-6.
14. Mu ZM, Xie YC, Peng XX, et al. Long-term survival after enucleation of a giant esophageal gastrointestinal stromal tumor. World J Gastroenterol 2014;20:13632-6.
15. Valls-Ferrusola E, García-Garzón JR, Ponce-López A, et al. Patterns of extension of gastrointestinal stromal tumors (GIST) treated with imatinib (Gleevec®) by 18F-FDG PET/CT. Rev Esp Enferm Dig 2012;104:360-6.
16. Farag S, Geus-Oei LF, van der Graaf WT, et al. Early Evaluation of Response Using 18F-FDG PET Influences Management in Gastrointestinal Stromal Tumor Patients Treated with Neoadjuvant Imatinib. J Nucl Med 2018;59:194-6.
17. Jerusalem G, Hustinx R, Beguin Y, et al. PET scan imaging in oncology. Eur J Cancer 2003;39:1525-34.
18. Kamiyama Y, Aihara R, Nakabayashi T, et al. 18F-fluorodeoxyglucose positron emission tomography: useful technique for predicting malignant potential of gastrointestinal stromal tumors. World J Surg 2005;29:1429-35.
19. Park JW, Cho CH, Jeong DS, et al. Role of F-fluoro-2-deoxyglucose Positron Emission Tomography in Gastric GIST: Predicting Malignant Potential Pre-operatively. J Gastric Cancer 2011;11:173-9.
20. Yoshikawa K, Shimada M, Kurita N, et al. Efficacy of PET-CT for predicting the malignant potential of gastrointestinal stromal tumors. Surg Today 2013;43:1162-7.
21. Cho MH, Park CK, Park M, et al. Clinicopathologic Features and Molecular Characteristics of Glucose Metabolism Contributing to ^{18}F-fluorodeoxyglucose Uptake in Gastrointestinal Stromal Tumors. PLoS One 2015;10:e0141413.
22. Tokumoto N, Tanabe K, Misumi T, et al. The usefulness of preoperative 18FDG positron-emission tomography and computed tomography for predicting the malignant

potential of gastrointestinal stromal tumors. Dig Surg 2014;31:79-86.
23. Belev B, Brčić I, Prejac J, et al. Role of Ki-67 as a prognostic factor in gastrointestinal stromal tumors. World J Gastroenterol 2013;19:523-7.
24. Zhao WY, Xu J, Wang M, et al. Prognostic value of Ki67 index in gastrointestinal stromal tumors. Int J Clin Exp Pathol 2014;7:2298-304.
25. Yamamoto H, Oda Y. Gastrointestinal stromal tumor: recent advances in pathology and genetics. Pathol Int 2015;65:9-18.
26. Choi SJ, Lee KH, Yoo CK, et al. Is There Pathological Uniformity between the Periphery and Center of a Gastrointestinal Stromal Tumor? J Clin Med 2021;10:687.
27. Lasota J, Miettinen M. Clinical significance of oncogenic KIT and PDGFRA mutations in gastrointestinal stromal tumours. Histopathology 2008;53:245-66.
28. Hwang SH, Jung M, Jeong YH, et al. Prognostic value of metabolic tumor volume and total lesion glycolysis on preoperative 18F-FDG PET/CT in patients with localized primary gastrointestinal stromal tumors. Cancer Metab 2021;9:8.

(English Language Editor: R. Scott)

Cite this article as: Li S, Lin D, Tang M, Liu D, Lyu Q, Zhang J. Value of ^{18}F-FDG PET/CT for differentiating diagnosis between malignant and benign primary gastric gastrointestinal mesenchymal tumors: a single-center retrospective study. J Gastrointest Oncol 2022;13(2):637-646. doi: 10.21037/jgo-22-287

